

# Demonstration of a Quantum Circuit Design Methodology for Multiple Regression\*

Sanchayan Dutta<sup>1,†</sup>, Adrien Suau<sup>2,‡</sup>, Sagnik Dutta<sup>3,§</sup>, Suvadeep Roy<sup>3,¶</sup>

Bikash K. Behera<sup>3,\*\*</sup> and Prasanta K. Panigrahi<sup>3,††</sup>

<sup>1</sup>*Department of Electronics and Telecommunication Engineering,  
Jadavpur University, Kolkata 700032, West Bengal, India*

<sup>2</sup>*CERFACS, 42 Avenue Gaspard Coriolis, 31100 Toulouse, France and*

<sup>3</sup>*Department of Physical Sciences, Indian Institute of Science Education  
and Research Kolkata, Mohanpur 741246, West Bengal, India*

## Abstract

Multiple linear regression, one of the most fundamental *supervised learning* algorithms, assumes an imperative role in the field of machine learning. In 2009, Harrow *et al.* [Phys. Rev. Lett. **103**, 150502 (2009)] showed that their algorithm could be used to *sample* the solution of a linear system  $\mathbf{Ax} = \mathbf{b}$  exponentially faster than any existing classical algorithm. Remarkably, any multiple linear regression problem can be reduced to a linear system of equations problem. However, finding a practical and efficient quantum circuit for the quantum algorithm in terms of elementary gate operations is still an open topic. Here we put forward a 7-qubit quantum circuit design, based on an earlier work by Cao *et al.* [Mol. Phys. **110**, 1675 (2012)], to solve a 3-variable regression problem, utilizing only basic quantum gates. Furthermore, we discuss the results of the Qiskit simulation for the circuit and explore certain possible generalizations to the circuit.

## I. Introduction

Quantum algorithms running on quantum computers aim at quickly and efficiently solving several important computational problems faster than classical algorithms running on classical computers [1–11]. One key way in which quantum algorithms differ from classical algorithms is that they utilize quantum mechanical phenomena such as superposition and entanglement, which allow us to work in exponentially large Hilbert spaces with only polynomial overheads. This in turn, in some cases, allows for exponential speed-ups in terms of algorithmic complexity [1].

In today’s world, machine learning is primarily concerned with the development of low-error models in order to make accurate predictions possible by learning and inferring from training data [12, 13]. It borrows heavily from the field of statistics in which linear regression is one of the flagship tools. The theory of multiple linear regression or more generally multivariate linear regression was largely developed in the field of statistics in the pre-computer era. It is one of the most well understood, versatile and straightforward techniques in any statistician’s toolbox. It is also an important and practical *supervised learning* algorithm. Supervised learning is where one has some labelled input data samples  $\{\mathbf{x}_i, \mathbf{y}_i\}_{i=1}^N$  (where  $\mathbf{x}_i$ ’s are the feature vectors and  $\mathbf{y}_i$ ’s are the corresponding labels) and then based on some criteria (which might depend on the context) chooses a mapping from input set  $\mathbf{X}$

to the output set  $\mathbf{Y}$ . And that mapping can help to predict the probable output corresponding to an input lying outside of the training data sets. Multiple linear regression is similar in the sense that given some training samples one identifies a closely-fitting *hyperplane* depending on the specific choice of a *loss function* (the most common one being a quadratic loss function based on the “least squares” method). Interestingly, any multiple regression problem can be converted into an equivalent system of linear equations problem or more specifically, a Quantum Linear Systems Problem (QLSP) problem [14]. The process has been outlined using an example in Section III.

Suppose that we are given a system of  $N$  linear equations with  $N$  unknowns, which can be expressed as  $\mathbf{Ax} = \mathbf{b}$ . Now, what we are interested in, is: given a matrix  $\mathbf{A} \in \mathbb{C}^{N \times N}$  with a vector  $\mathbf{b} \in \mathbb{C}^N$ , find the solution  $\mathbf{x} \in \mathbb{C}^N$  satisfying  $\mathbf{Ax} = \mathbf{b}$  (which is  $\mathbf{A}^{-1}\mathbf{b}$  if  $\mathbf{A}$  is invertible), or else return a *flag* if no solution exists. This is known as the Linear Systems Problem (LSP). However, we will consider only a special case of this general problem, in form of the Quantum Linear Systems Problem (QLSP) [14, 15].

The quantum version of the LSP problem, that is, the QLSP can be expressed as:

*Let  $\mathbf{A}$  be a  $N \times N$  Hermitian matrix with a spectral norm bounded by unity and a known condition number  $\kappa$ . The quantum state on  $\lceil \log N \rceil$  qubits  $|b\rangle$  can be given by*

$$|b\rangle := \frac{\sum_i b_i |i\rangle}{\|\sum_i b_i |i\rangle\|} \quad (1)$$

and  $|x\rangle$  by

$$|x\rangle := \frac{\sum_i x_i |i\rangle}{\|\sum_i x_i |i\rangle\|} \quad (2)$$

\* These authors contributed equally to the work:

† [sanchayan98@gmail.com](mailto:sanchayan98@gmail.com)

‡ [adrien.suau@cerfacs.fr](mailto:adrien.suau@cerfacs.fr)

§ [sd15ms136@iiserkol.ac.com](mailto:sd15ms136@iiserkol.ac.com)

¶ [sr15ms116@iiserkol.ac.com](mailto:sr15ms116@iiserkol.ac.com);

These authors supervised the project:

\*\* [bkb18rs025@iiserkol.ac.in](mailto:bkb18rs025@iiserkol.ac.in)

†† [pprasanta@iiserkol.ac.in](mailto:pprasanta@iiserkol.ac.in)

where  $b_i, x_i$  are respectively the  $i^{\text{th}}$  component of vectors  $\mathbf{b}$  and  $\mathbf{x}$ . Given the matrix  $\mathbf{A}$  (whose elements are accessed by an oracle) and the state  $|b\rangle$ , an output state  $|\tilde{x}\rangle$  is such that  $\| |\tilde{x}\rangle - |x\rangle \|_2 \leq \epsilon$ , with some probability  $\Omega(1)$  (practically at least  $\frac{1}{2}$ ) along with a binary flag indicating ‘success’ or ‘failure’ [14].

The restrictions on Hermiticity and spectral norm, can be relaxed by noting that, even for a non-Hermitian matrix  $A$ , the corresponding  $\begin{bmatrix} 0 & \mathbf{A}^\dagger \\ \mathbf{A} & 0 \end{bmatrix}$  matrix is Hermitian. This implies that we can instead solve the linear system given by  $\begin{bmatrix} 0 & \mathbf{A}^\dagger \\ \mathbf{A} & 0 \end{bmatrix} \mathbf{y} = \begin{bmatrix} \mathbf{b} \\ 0 \end{bmatrix}$ , which has the unique solution  $\mathbf{y} = \begin{bmatrix} 0 \\ \mathbf{x} \end{bmatrix}$  when  $\mathbf{A}$  is invertible [4]. Also, any non-singular matrix can be scaled appropriately to adhere to the given conditions on the eigenspectrum. Note that the case when  $A$  is non-invertible, has already been excluded by the fact that a known finite condition number exists for the matrix  $\mathbf{A}$ .

In 2009, A. W. Harrow, A. Hassidim and S. Lloyd [4] put forward a quantum algorithm (popularly known as the “HHL algorithm”) to obtain information about the solution  $\mathbf{x}$  of certain classes of linear systems  $\mathbf{A}\mathbf{x} = \mathbf{b}$ . As we know, algorithms for finding the solutions to linear systems of equations play an important role in engineering, physics, chemistry, computer science, and economics apart from other areas. However, experimentally implementing the HHL algorithm for solving an arbitrary system of linear equations to a satisfactory degree of accuracy, remains an infeasible task even today, due to several physical and theoretical restrictions imposed by the algorithm and the currently accessible hardware. It is therefore imperative to extract as much practical benefit as we can from the algorithm. In Section IV, we present an application (in the context of multiple regression) of a modified version of the earlier circuit design by Cao *et al.* [18] which was meant for implementing the HHL algorithm for a  $4 \times 4$  linear system on real quantum computers. This circuit requires only 7 qubits and it should be simple enough to experimentally verify it, one gets access to quantum computers with quantum logic gates with sufficiently low error rates. Previously, Pan *et al.* demonstrated the HHL on a 4-qubit NMR quantum computer [17], so we believe that it will be easily possible to experimentally implement the circuit we discuss, given the rapid rise in the number of qubits in quantum computer chips, in the past few years.

Although the HHL solves the QLSP for all such matrices  $\mathbf{A}$  or  $\begin{bmatrix} 0 & \mathbf{A}^\dagger \\ \mathbf{A} & 0 \end{bmatrix}$ , it can be efficiently implemented only when they are sparse and well-conditioned (the sparsity condition may be slightly relaxed) [14]. In this context, ‘efficient’ means ‘at most poly-logarithmic in system size’. A  $N \times N$  matrix is called *s-sparse* if it has at most  $s$  non-zero entries in any row or column. We call it simply *sparse* if it has at most  $\text{poly}(\log N)$  entries per row [15]. We generally call a matrix well-conditioned when its singular values lie between the reciprocal of its condition number ( $\frac{1}{\kappa}$ ) and 1 [4]. *Condition number*  $\kappa$  of a matrix is the ratio of largest to smallest singular value and is undefined when the smallest singular value of  $\mathbf{A}$  is

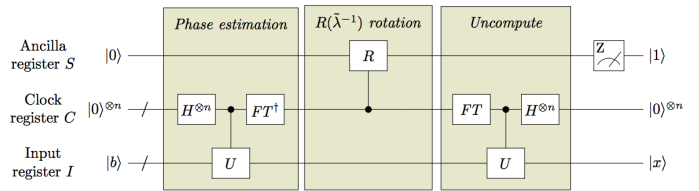


FIG. 1. HHL Algorithm Schematic <sup>1</sup>

0. For Hermitian matrices the magnitude of the eigenvalues are equal to the magnitudes of the respective singular values.

At this point it is important to reiterate that unlike the output  $\mathbf{A}^{-1}\mathbf{b}$  of a classical linear system solver, the output copy of  $|\tilde{x}\rangle$  does not provide access to the coordinates of  $\mathbf{A}^{-1}\mathbf{b}$ . Nevertheless, it allows for *sampling* from the solution vectors like  $\langle \tilde{x} | M | \tilde{x} \rangle$ , where  $M$  is a quantum-mechanical operator. This is one main difference between solutions of the LSP and solutions of the QLSP. We should also keep in mind that reading out the elements of  $|\tilde{x}\rangle$  in itself takes  $\mathcal{O}(N)$  time. Thus, a solution to QLSP might be useful only in applications where just samples from the vector  $|\tilde{x}\rangle$  are needed [4, 14, 15].

The best existing classical matrix inversion algorithm involves the Gaussian elimination technique which takes  $\mathcal{O}(N^3)$  time. For  $s$ -sparse and positive semi-definite  $A$ , the Conjugate Gradient algorithm [19] can be used to find the solution vector  $\mathbf{x}$  in  $\mathcal{O}(Ns\kappa \log(1/\epsilon))$  time by minimizing the quadratic error function  $|\mathbf{A}\mathbf{x} - \mathbf{b}|^2$ , where  $s$  is the matrix sparsity,  $\kappa$  is the condition number and  $\epsilon$  is the desired precision parameter. On the other hand, the HHL algorithm scales as  $\mathcal{O}(\log(N)s^2\kappa^2/\epsilon)$ , and is exponentially faster in  $N$  but polynomially slower in  $s$  and  $\kappa$ . In 2010, Andris Ambainis further improved the runtime of the HHL to  $\mathcal{O}(\kappa \log^3 \kappa \log N/\epsilon)$  [20]. The exponentially worse slowdown in  $\epsilon$  was also eliminated [14] by Childs *et al.* in 2017 and it got improved to  $\mathcal{O}(s\kappa \text{polylog}(s\kappa/\epsilon))$  [15]. Since the HHL has logarithmic scaling only for sparse or low rank matrices, in 2018, Wossnig *et al.* extended the HHL algorithm with quantum singular value estimation and provided a quantum linear system algorithm for dense matrices which achieves a polynomial improvement in time complexity, that is,  $\mathcal{O}(\sqrt{N} \text{polylog}(N)\kappa^2/\epsilon)$  [21] (the HHL retains its logarithmic scaling only for sparse or low rank matrices). Furthermore, an exponential improvement is achievable with this algorithm if the rank of  $\mathbf{A}$  is polylogarithmic in the matrix dimension.

Last but not the least, we note that it is assumed that the state  $|b\rangle$  can be efficiently constructed i.e., prepared in ‘poly-logarithmic time’. In reality, however, efficient preparation of arbitrary quantum states is too hard, and is subject to several constraints.

## II. The Harrow Hassidim Lloyd Algorithm

The HHL algorithm consists of three major steps which we will briefly discuss one by one. Initially, we begin with a Hermitian matrix  $\mathbf{A}$  and an input state  $|b\rangle$  corresponding to our specific system of linear equations. The assumption that  $\mathbf{A}$  is Hermitian may be dropped without loss of generality since we can instead solve the linear system of equations given by  $\begin{bmatrix} 0 & \mathbf{A}^\dagger \\ \mathbf{A} & 0 \end{bmatrix} \mathbf{y} = \begin{bmatrix} \mathbf{b} \\ 0 \end{bmatrix}$  which has the unique solution  $\mathbf{y} = \begin{bmatrix} 0 \\ \mathbf{x} \end{bmatrix}$  when  $\mathbf{A}$  is invertible. This transformation does not alter the condition number (ratio of the magnitudes of the largest and smallest eigenvalues) of  $\mathbf{A}$  [4, 14]. However, in the case our original matrix  $\mathbf{A}$  is not Hermitian, the transformed system with the new matrix  $\begin{bmatrix} 0 & \mathbf{A}^\dagger \\ \mathbf{A} & 0 \end{bmatrix}$  needs oracle access to the non-zero entries of the rows *and* columns of  $\mathbf{A}$  [14]. Since  $\mathbf{A}$  is assumed to be Hermitian, it follows that  $e^{i\mathbf{A}t}$  is unitary. Here  $i\mathbf{A}t$  and  $-i\mathbf{A}t$  commute and hence  $e^{i\mathbf{A}t}e^{-i\mathbf{A}t} = e^{i\mathbf{A}t-i\mathbf{A}t} = e^0 = \mathbf{I}$ . Moreover,  $e^{i\mathbf{A}t}$  shares all its eigenvectors with  $\mathbf{A}$ , while it's eigenvalues are  $e^{i\lambda_j t}$  if the eigenvalues of  $\mathbf{A}$  are taken to be  $\lambda_j$ . Suppose that  $|u_j\rangle$  are the eigenvectors of  $\mathbf{A}$  and  $\lambda_j$  are the corresponding eigenvalues. We recall that we assumed all the eigenvalues to be of magnitude less than 1 (spectral norm is bounded by unity). As the eigenvalues  $\lambda_j$  are of the form  $0.a_1a_1a_3\dots$  in binary [1, p. 222], we will use  $|\lambda_j\rangle$  to refer to  $|a_1a_2a_3\dots\rangle$ . We know from the spectral theorem that every Hermitian matrix has an orthonormal basis of eigenvectors. So, in this context,  $\mathbf{A}$  can be re-written as  $\sum_j \lambda_j |u_j\rangle\langle u_j|$  (via eigendecomposition of  $\mathbf{A}$ ) and  $|b\rangle$  as  $\sum_j \beta_j |u\rangle_j$ .

### A. Phase Estimation

The quantum phase estimation algorithm performs the mapping  $(|0\rangle^{\otimes n})^C |u\rangle^I |0\rangle^S \mapsto |\tilde{\varphi}\rangle^C |u\rangle^I |0\rangle^S$  where  $|u\rangle$  is an eigenvector of a unitary operator  $U$  with an unknown eigenvalue  $e^{i2\pi\varphi}$  [1].  $\tilde{\varphi}$  is a  $t$ -bit approximation of  $\varphi$ , where  $t$  is the number of qubits in the clock register. The superscripts on the kets indicate the names of the registers which store the corresponding states. In the HHL algorithm the input register begins with a superposition of eigenvectors instead i.e.,  $|b\rangle = \sum_j \beta_j |u_j\rangle$  instead of a specific eigenvector  $|u\rangle$ , and for us the unitary operator is  $e^{i\mathbf{A}t}$ . So the phase estimation circuit performs the mapping

$$\left(|0\rangle^{\otimes n}\right)^C |b\rangle^I \mapsto \left(\sum_{j=1}^N \beta_j |u_j\rangle^I \left|\frac{\tilde{\lambda}_j t_0}{2\pi}\right\rangle^C\right)$$

<sup>1</sup> The HHL algorithm schematic (Fig. 1) was generated using the TikZ code provided by Dr. Niel de Beaudrap (Department of Computer Science, Oxford University). It was inspired by figure 5 of the Dervovic *et al.* paper [15].

where  $\tilde{\lambda}_j$ 's are the binary representations of the eigenvalues of  $\mathbf{A}$  to a tolerated precision. To be more explicit, here  $\tilde{\lambda}_j$  is represented as  $b_1b_2b_3\dots b_t$  ( $t$  is the number of qubits in the clock register) if the actual binary equivalent of  $\lambda_j$  is of the form  $\lambda = 0.b_1b_2b_3\dots$ . To avoid the factor of  $2\pi$  in the denominator, the 'evolution time'  $t_0$  is generally chosen to be  $2\pi$ . However,  $t_0$  may also be used to 'normalize'  $\mathbf{A}$  (by re-scaling  $t_0$ ) in case the spectral norm of  $A$  exceeds  $1^2$ . Additionally, an important factor in the performance of the algorithm is the condition number  $\kappa$ . As  $\kappa$  grows,  $\mathbf{A}$  tends more and more towards a non-invertible matrix, and the solutions become less and less stable [4]. Matrices with large condition numbers are said to be 'ill-conditioned'. The HHL algorithm generally assumes that the singular values of  $\mathbf{A}$  lie between  $1/\kappa$  and 1, which ensures that the matrices we have to deal with are 'well-conditioned'. Nonetheless, there are methods to tackle ill-conditioned matrices and those have been thoroughly discussed in the paper by Lloyd *et al.* [4]. It is worth mentioning that in this step the 'clock register'-controlled Hamiltonian simulation gate  $U$  can be expressed as  $\sum_{k=0}^{T-1} |\tau\rangle\langle\tau|^C \otimes e^{i\mathbf{A}\tau t_0/T}$ , where  $T = 2^t$  ( $t$  is the number of qubits in the clock register) and evolution time  $t_0 = \mathcal{O}(\kappa/\epsilon)$ . Interestingly choosing  $t_0 = \mathcal{O}(\kappa/\epsilon)$  can at maximum error cause an error of magnitude  $\epsilon$  in the final state [4].

### B. $\mathbf{R}(\tilde{\lambda}^{-1})$ rotation

A 'clock register' controlled  $\sigma_y$ -rotation of the 'ancilla' qubit produces a normalized state of the form

$$\sum_{j=1}^N \beta_j |u_j\rangle^I \left|\tilde{\lambda}_j\right\rangle^C \left(\sqrt{1 - \frac{C^2}{\tilde{\lambda}_j^2}} |0\rangle + \frac{C}{\tilde{\lambda}_j} |1\rangle\right)^S$$

These rotations, conditioned on respective  $\tilde{\lambda}_j$ , can be achieved by the application of the  $\exp(-i\theta\sigma_y) = \begin{bmatrix} \cos\theta & -\sin\theta \\ \sin\theta & \cos\theta \end{bmatrix}$  operators where  $\theta = \cos^{-1}\left(\frac{C}{\tilde{\lambda}_j}\right)$ .  $C$  is a scaling factor to prevent the controlled rotation from being unphysical [15]. That is, practically  $C < \lambda_{\min}$  (minimum eigenvalue of  $\mathbf{A}$ ) is a safe choice, which may be more formally stated as  $C = \mathcal{O}(1/\kappa)$  [4].

### C. Uncomputation

In the final step, the inverse quantum phase estimation algorithm sets back the clock register to  $(|0\rangle^{\otimes n})^C$  and

<sup>2</sup> Ideally, we should know both the upper bound and the lower bound of the eigenvalues, for effective rescaling. Furthermore, to get accurate estimates, we should attempt to spread the possible values of  $\lambda t$  over the whole  $2\pi$  range.

leaves the remaining state as

$$\sum_{j=1}^N \beta_j |u_j\rangle^I \left( \sqrt{1 - \frac{C^2}{\lambda_j^2}} |0\rangle + \frac{C}{\lambda_j} |1\rangle \right)^S$$

Postselecting on the ancilla  $|1\rangle^S$  gives the final state  $C \sum_{j=1}^N (\frac{\beta_j}{\lambda_j}) |u_j\rangle^I$  [15]. The inverse of the Hermitian matrix  $\mathbf{A}$  can be written as  $\sum_j \frac{1}{\lambda_j} |u_j\rangle \langle u_j|$ , and hence  $\mathbf{A}^{-1}|b\rangle$  matches  $\sum_{j=1}^N \frac{\beta_j}{\lambda_j} |u_j\rangle^I$ . This outcome state, in the standard basis, is component-wise proportional to the exact solution  $\mathbf{x}$  of the system  $\mathbf{A}\mathbf{x} = \mathbf{b}$  [18].

### III. Linear Regression Utilizing the HHL

Linear regression models a linear relationship between a scalar ‘response’ variable and one or more ‘feature’ variables. Given a  $n$ -unit data set  $\{y_i, x_{i1}, \dots, x_{ip}\}_{i=1}^n$ , a linear regression model assumes that the relationship between the dependent variable  $y$  and a set of  $p$  attributes i.e.,  $\mathbf{x} = \{x_1, \dots, x_p\}$  is linear [12]. Essentially, the model takes the form

$$y_i = \beta_0 + \beta_1 x_{i1} + \dots + \beta_p x_{ip} + \epsilon_i = \mathbf{x}_i^T \boldsymbol{\beta} + \epsilon_i$$

where  $\epsilon_i$  is the noise or error term. Here  $i$  ranges from 1 to  $n$ .  $\mathbf{x}_i^T$  denotes the transpose of the column matrix  $\mathbf{x}_i$ . And  $\mathbf{x}_i^T \boldsymbol{\beta}$  is the *inner product* between vectors  $\mathbf{x}_i$  and  $\boldsymbol{\beta}$ . These  $n$  equations may be more compactly represented in the matrix notation, as  $\mathbf{y} = \mathbf{X}\boldsymbol{\beta} + \boldsymbol{\epsilon}$ . Now, we will consider a simple example with 3 feature variables and a bias  $\beta_0$ . Say our data sets are  $\{-\frac{1}{8} + \frac{1}{8\sqrt{2}}, -\sqrt{2}, \frac{1}{\sqrt{2}}, -\frac{1}{2}\}$ ,  $\{\frac{3}{8} - \frac{3}{8\sqrt{2}}, -\sqrt{2}, -\frac{1}{\sqrt{2}}, \frac{1}{2}\}$ ,  $\{-\frac{1}{8} - \frac{1}{8\sqrt{2}}, \sqrt{2}, -\frac{1}{\sqrt{2}}, -\frac{1}{2}\}$  and  $\{\frac{3}{8} + \frac{3}{8\sqrt{2}}, \sqrt{2}, \frac{1}{\sqrt{2}}, \frac{1}{2}\}$ . Plugging in these data sets we get the linear system:

$$\beta_0 - \sqrt{2}\beta_1 + \frac{1}{\sqrt{2}}\beta_2 - \frac{1}{2}\beta_3 = -\frac{1}{8} + \frac{1}{8\sqrt{2}} \quad (3)$$

$$\beta_0 - \sqrt{2}\beta_1 - \frac{1}{\sqrt{2}}\beta_2 + \frac{1}{2}\beta_3 = \frac{3}{8} - \frac{3}{8\sqrt{2}} \quad (4)$$

$$\beta_0 + \sqrt{2}\beta_1 - \frac{1}{\sqrt{2}}\beta_2 - \frac{1}{2}\beta_3 = -\frac{1}{8} - \frac{1}{8\sqrt{2}} \quad (5)$$

$$\beta_0 + \sqrt{2}\beta_1 + \frac{1}{\sqrt{2}}\beta_2 + \frac{1}{2}\beta_3 = \frac{3}{8} + \frac{3}{8\sqrt{2}} \quad (6)$$

To estimate  $\boldsymbol{\beta}$  we will use the popular ‘least squares’ method, which minimizes the residual sum of squares  $\sum_{i=1}^N (y_i - \mathbf{x}_i \boldsymbol{\beta}_i)^2$ . If  $\mathbf{X}$  is *positive definite* (and in turn has *full rank*) we can obtain a unique solution for the best fit  $\hat{\boldsymbol{\beta}}$ , which is  $(\mathbf{X}^T \mathbf{X})^{-1} \mathbf{X}^T \mathbf{y}$ . It is possible that all

the columns of  $\mathbf{X}$  are not linearly independent and by extension  $\mathbf{X}$  is not full rank. This kind of a situation might occur if two or more of the feature variables are perfectly correlated. Then  $\mathbf{X}^T \mathbf{X}$  would be singular and  $\hat{\boldsymbol{\beta}}$  wouldn’t be uniquely defined. Nevertheless, there exist techniques like ‘filtering’ to resolve the non-unique representations by reducing the redundant features. Rank deficiencies might also occur if the number of features  $p$  exceed the number of data sets  $N$ . If we estimate such models using ‘regularization’, then redundant columns should not be left out. The regulation takes care of the singularities. More importantly, the final prediction might depend on which columns are left out [22].

Equations (3)-(6) may be expressed in the matrix notation as:

$$\begin{bmatrix} -\sqrt{2} & 1 & \frac{1}{\sqrt{2}} & -\frac{1}{2} \\ -\sqrt{2} & 1 & -\frac{1}{\sqrt{2}} & \frac{1}{2} \\ -\sqrt{2} & -1 & \frac{1}{\sqrt{2}} & \frac{1}{2} \\ \sqrt{2} & 1 & \frac{1}{\sqrt{2}} & \frac{1}{2} \end{bmatrix} \begin{bmatrix} \beta_1 \\ \beta_0 \\ \beta_1 \\ \beta_2 \end{bmatrix} = \begin{bmatrix} -\frac{1}{8} + \frac{1}{8\sqrt{2}} \\ \frac{3}{8} - \frac{3}{8\sqrt{2}} \\ \frac{1}{8} + \frac{1}{8\sqrt{2}} \\ \frac{3}{8} + \frac{3}{8\sqrt{2}} \end{bmatrix} \quad (7)$$

Note that unlike common convention, our representation of  $\mathbf{X}$  does not contain a column full of 1’s corresponding the bias term. This representation is used simply because of the convenient form which we obtain for  $\mathbf{X}^T \mathbf{X}$ . The final result remains unaffected as long as  $\mathbf{y} = \mathbf{X}\boldsymbol{\beta}$  represents the same linear system.

Now

$$\mathbf{X}^T \mathbf{X} = \frac{1}{4} \begin{bmatrix} 15 & 9 & 5 & -3 \\ 9 & 15 & 3 & -5 \\ 5 & 3 & 15 & -9 \\ -3 & -5 & -9 & 15 \end{bmatrix} \quad (8)$$

and

$$\mathbf{X}^T \mathbf{y} = \begin{bmatrix} \frac{1}{2} \\ \frac{1}{2} \\ \frac{1}{2} \\ \frac{1}{2} \end{bmatrix}. \quad (9)$$

Thus we need to solve for  $\hat{\boldsymbol{\beta}}$  from  $\mathbf{X}^T \mathbf{X} \hat{\boldsymbol{\beta}} = \mathbf{X}^T \mathbf{y}$  [12].

### IV. Quantum Circuit

Having discussed the general idea behind the HHL algorithm in Section II and its possible application in drastically speeding up multiple regression in Section III, we now move on to the quantum circuit design meant to solve the  $4 \times 4$  linear system which we encountered in Section III i.e.,  $\mathbf{X}^T \mathbf{X} \hat{\boldsymbol{\beta}} = \mathbf{X}^T \mathbf{y}$ . For sake of convenience we will now denote  $\mathbf{X}^T \mathbf{X}$  with  $\mathbf{A}$ ,  $\hat{\boldsymbol{\beta}}$  with  $\mathbf{x}$  and  $\mathbf{X}^T \mathbf{y}$  with  $\mathbf{b}$ . The circuit requires only 7 qubits, with 4 qubits

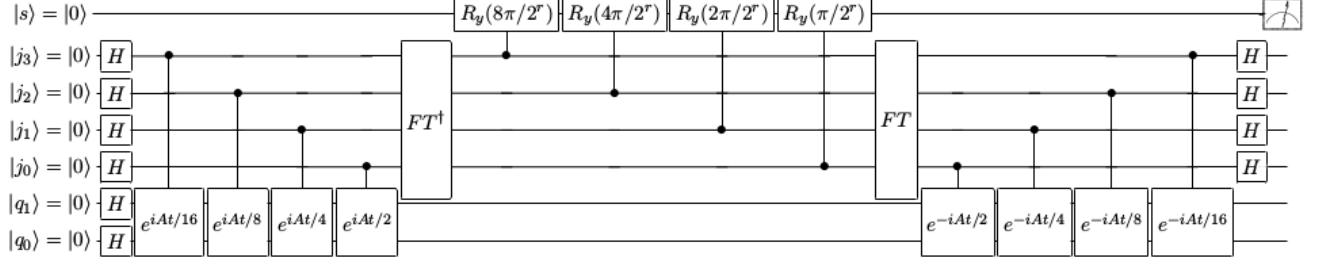


FIG. 2. Quantum circuit for solving a  $4 \times 4$  system of linear equation  $\mathbf{Ax} = \mathbf{b}$ . The top qubit ( $|s\rangle$ ) is the ancilla qubit. The four qubits in the middle ( $|j_0\rangle, |j_1\rangle, |j_2\rangle$  and  $|j_3\rangle$ ) stand for the Clock register  $C$ . The two qubits at the bottom ( $|q_0\rangle$  and  $|q_1\rangle$ ) form the Input register  $I$  and two Hadamard gates are applied on them to initialize the state  $|b\rangle$

in the “clock register”, 2 qubits in the “input register” and remaining 1 as an “ancilla” qubit. At this point it is imperative to mention that we specifically chose the form of the regression data points in the previous Section such that  $\mathbf{A}$  turns out to be Hermitian, has four distinct eigenvalues of the form  $\lambda_i = 2^{i-1}$  and  $\mathbf{b}$  has a convenient form which can be efficiently prepared by simply using two Hadamard gates.

$$\mathbf{A} = \frac{1}{4} \begin{bmatrix} 15 & 9 & 5 & -3 \\ 9 & 15 & 3 & -5 \\ 5 & 3 & 15 & -9 \\ -3 & -5 & -9 & 15 \end{bmatrix} \quad (10)$$

$\mathbf{A}$  is a Hermitian matrix with eigenvalues  $\lambda_1 = 1, \lambda_2 = 2, \lambda_3 = 4$  and  $\lambda_4 = 8$ . The corresponding eigenvectors encoded in quantum states  $|u_j\rangle$  may be expressed as

$$|u_1\rangle = -|00\rangle - |01\rangle - |10\rangle + |11\rangle \quad (11)$$

$$|u_2\rangle = +|00\rangle + |01\rangle - |10\rangle + |11\rangle \quad (12)$$

$$|u_3\rangle = +|00\rangle - |01\rangle + |10\rangle + |11\rangle \quad (13)$$

$$|u_4\rangle = -|00\rangle + |01\rangle + |10\rangle + |11\rangle \quad (14)$$

Also,  $\mathbf{b} = \left[ \frac{1}{2} \ \frac{1}{2} \ \frac{1}{2} \ \frac{1}{2} \right]^T$  can be written as  $\sum_{j=1}^{j=4} \beta_j |u_j\rangle$  where each  $\beta_j = \frac{1}{2}$ .

We will now trace through the quantum circuit in Fig. 2.  $|q_0\rangle$  and  $|q_1\rangle$  are the input register qubits which are initialized to a combined quantum state

$$|b\rangle = \frac{1}{2}|00\rangle + \frac{1}{2}|01\rangle + \frac{1}{2}|10\rangle + \frac{1}{2}|11\rangle \quad (15)$$

which is basically the state-encoded format of  $\mathbf{b}$ . This is followed by the quantum phase estimation step which involves a Walsh-Hadamard transform on the clock

register qubits  $|j_0\rangle, |j_1\rangle, |j_2\rangle, |j_3\rangle$ , a clock register controlled unitary gates  $U^{2^0}, U^{2^1}, U^{2^2}$  and  $U^{2^3}$  where  $U = \exp(i\mathbf{A}t/16)$  and an inverse quantum Fourier transform on the clock register. As discussed in Section II, this step would produce the state  $\frac{1}{2}|0001\rangle^C |u_1\rangle^I + \frac{1}{2}|0010\rangle^C |u_2\rangle^I + \frac{1}{2}|0100\rangle^C |u_3\rangle^I + \frac{1}{2}|1000\rangle^C |u_4\rangle^I$ , which is essentially the same as  $\sum_{j=1}^N \beta_j |u_j\rangle^I \left| \frac{\tilde{\lambda}_j t_0}{2\pi} \right\rangle^C$ , assuming  $t_0 = 2\pi$ . Also, in this specific example  $|\tilde{\lambda}_j\rangle = |\lambda_j\rangle$ , since the 4 qubits in the clock register are sufficient to accurately and precisely represent the 4 eigenvalues in binary. As far as the endianness of the combined quantum states is concerned we must keep in mind that in our circuit  $|q_0\rangle$  is the *most significant* qubit (MSQ) and  $|q_3\rangle$  is the *least significant* qubit (LSQ).

Next is the  $R(\tilde{\lambda}^{-1})$  rotation step. We make use of an ancilla qubit  $|s\rangle$  (initialized in the state  $|0\rangle$ ), which gets phase shifted depending upon the clock register’s state. Let’s take an example clock register state  $|0100\rangle^C = |0\rangle_{q_0}^C \otimes |1\rangle_{q_1}^C \otimes |0\rangle_{q_2}^C \otimes |0\rangle_{q_3}^C$  (binary representation of the eigenvalue corresponding to  $|u_3\rangle$ , that is 4). In this combined state,  $|q_1\rangle$  is in the state  $|1\rangle$  while  $|q_0\rangle, |q_2\rangle$  and  $|q_3\rangle$  are all in the state  $|0\rangle$ . This state will only trigger the  $R_y(\frac{8\pi}{4 \cdot 2^r})$  rotation gate, and none of the other phase shift gates. Thus, we may say that the smallest eigenvalue states in  $C$  cause the largest ancilla rotations. Using linearity arguments, it is clear that if the clock register state had instead been  $|b\rangle$ , as in our original example, the final state generated by this rotation step would be  $\sum_{j=1}^N \beta_j |u_j\rangle^I \left| \frac{\tilde{\lambda}_j}{\lambda_j} \right\rangle^C \left( (1 - C^2/\tilde{\lambda}_j^2)^{1/2} |0\rangle + \frac{C}{\tilde{\lambda}_j} |1\rangle \right)^S$  where  $C = 8\pi/2^r$ . For this step, an a priori knowledge of the eigenvalues of  $\mathbf{A}$  was necessary to design the gates. For more general cases of eigenvalues, one may refer to [18].

Then, as elaborated in Section II, the inverse phase estimation step essentially reverses the quantum phase estimation step. The state produced by this step, conditioned on obtaining  $|1\rangle$  in ancilla is  $\frac{8\pi}{2^r} \sum_{j=1}^{j=4} \frac{1}{2^{j-1}} |u_j\rangle$ .

Upon writing in the standard basis and normalizing, it becomes  $\frac{1}{\sqrt{340}}(-|00\rangle + 7|01\rangle + 11|10\rangle + 13|11\rangle)$ . This is proportional to the exact solution of the system  $\mathbf{x} = \frac{1}{32}[-1 \ 7 \ 11 \ 13]^T$ .

## V. Simulation

We simulated the quantum circuit in Fig. 2 using Qiskit [16]. One of the main hurdles while implementing the quantum program was dealing with the Hamiltonian simulation step i.e., implementing the controlled unitary  $\mathbf{U} = e^{i\mathbf{A}t}$ . Taking a cue from the Cao *et al.* paper [18] which employed the Group Leaders Optimization algorithm (GLOA) [23], we approximately decomposed  $\mathbf{U}$  gates into elementary quantum gates, as shown in Fig. 3. It's however important to keep in mind that using the GLOA to decompose the  $\mathbf{U}$  is useful only when the matrix exponential  $e^{i\mathbf{A}t}$  is readily available. Let's call the resulting approximated unitary  $\tilde{\mathbf{U}}$ . The parameters of the  $R_x$  and  $R_{zz}$  gates given in [18] were refined using the `scipy.optimize.minimize` function [24], in order to minimize the Hilbert-Schmidt norm of  $\mathbf{U} - \tilde{\mathbf{U}}$  (which is a measure of the relative error between  $\mathbf{U}$  and  $\tilde{\mathbf{U}}$ ). The `scipy.optimize.minimize` function makes use of the quasi-Newton algorithm of Broyden, Fletcher, Goldfarb, and Shanno (BFGS) [25] by default. Also, we noticed that it is necessary to use a controlled- $Z$  gate instead of a single qubit  $Z$  gate (as in [18]).

A sample output of the QISKit code has been shown in the text-box (V). All the results have been rounded to 4 decimal places. The 'Error in found solution' is in essence the 2-norm of the difference between the exact solution and the output solution. We have neglected normalization and constant factors like  $\frac{1}{32}$  in the displayed solutions.

It is evident from the low error value, that the gate decomposition we used for  $\tilde{\mathbf{U}}$  helps to approximately replicate the ideal circuit involving  $\mathbf{U}$ . Also, the difference between the predicted and simulated results (with shots =  $10^5$ ) has been shown in Fig. 4.

Qiskit Simulation – Sample Output:

Predicted solution:

$[-1 \ 7 \ 11 \ 13]$

Experimental solution:

$[-0.8425 \ 6.9604 \ 10.9980 \ 13.0341]$

Error in found solution: 0.1660

One should remember that using stochastic genetic algorithms like the Group Leaders Optimization algorithm for the Hamiltonian simulation step is a viable technique only when cost of computing the matrix exponential  $e^{i\mathbf{A}t}$

is substantially lower than the cost of solving the corresponding system of linear system classically. A popular classical algorithm for calculating matrix exponentials is the 'The Scaling and Squaring Algorithm' by Al-Mohy and J. Higham [27, 28, 30], whose cost is  $\mathcal{O}(n^3)$ , and which is generally used along with the Padé approximation by Matlab [29] and SciPy [24]. But this algorithm is mostly used for small dense matrices. For large sparse matrices, better approaches exist. For instance, in the Krylov space approach [31][32], an Arnoldi algorithm is used whose cost is in the ballpark of  $\mathcal{O}(mn)$ , where  $n$  is the matrix size and  $m$  is the number of Krylov vectors which need to be computed. In general, for large sparse matrices the GLOA may be useful but that decision needs to be made on a case-by-case basis depending on the properties of the particular matrix  $\mathbf{A}$  which one is dealing with.

## VI. Conclusion

To conclude, we have noticed that any multiple regression problem can be reduced to an equivalent linear system of equations problem. This allows us to employ the general quantum speed-up techniques like the HHL algorithm. However, for the HHL we need low error low cost circuits for the Hamiltonian simulation and controlled rotation steps to get accurate results. Although methods like Trotter-Suzuki decomposition and the Solvay-Kitaev algorithm can help to decompose Hamiltonian simulation, but except in certain cases they provide neither minimum cost nor efficient gate sequences. In most practical scenarios we would prefer a low cost gate sequence which approximates the unitary operator well, rather than a high cost exact decomposition. This is where stochastic genetic algorithms like the GLOA comes into play. However, we noted earlier, the GLOA turns out to be useful only in those cases where the matrix exponentials can be efficiently calculated. Otherwise the speedup provided by the HHL would be nullified. One might also argue that the large time taken to find the correct set of gates for the HHL, given a particular  $\mathbf{A}$ , renders the quantum speed-up achieved useless. That is indeed true for smaller datasets but one should recall that the discussed technique reveals its true speed-up only for large datasets. This is because we restrict the number of gates to be used for the GLOA to a maximum of 20 (as discussed in the appendix). So while the number and size of the data sets can be arbitrarily large, only a limited number of gates will ever be used for approximating the Hamiltonian simulation step of the HHL.

## VII. Acknowledgements

Sanchayan Dutta would like to thank IISER Kolkata for providing hospitality and support during the period of the Summer Student Research Program (2018). Adrien Suau acknowledges the support provided by CERFACS. Suvadeep Roy and Sagnik Dutta are obliged to INSPIRE,

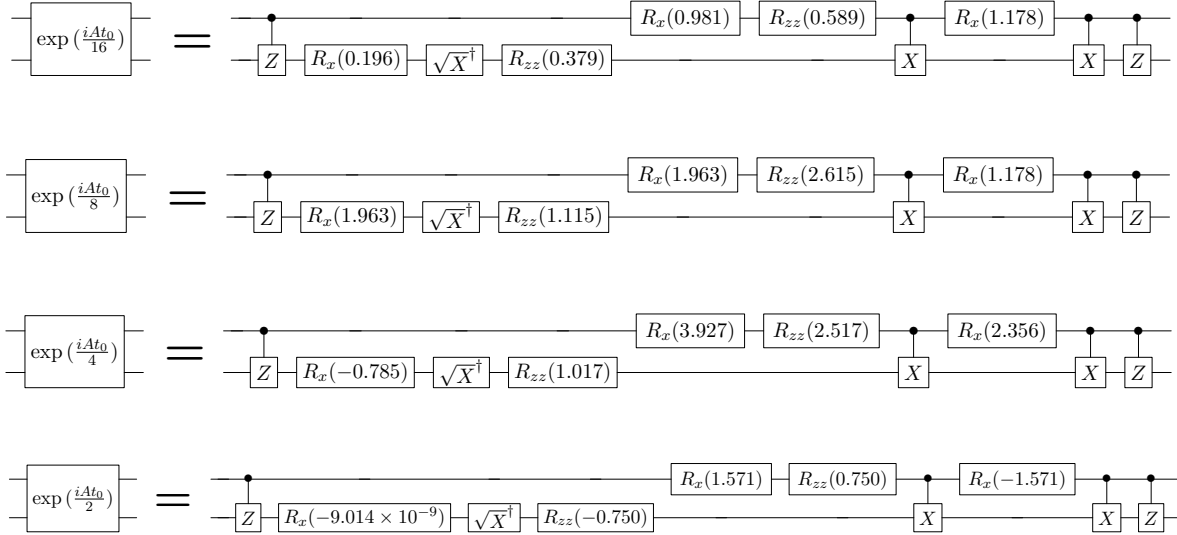


FIG. 3. The Group Leaders Optimization Algorithm is employed to approximately decompose the  $\exp\left(\frac{iAt}{2^k}\right)$  gates in the Hamiltonian simulation step into elementary quantum gates. The decomposition is not unique. The specific gate decompositions shown in the diagram were taken Cao *et al.*[18] and the angle shifts were corrected using the *scipy.optimize.minimize* module.  $\exp\left(\frac{iAt}{2^k}\right)$  gates.



FIG. 4. The blue bars represent the predicted or expected state amplitudes for the solution vector  $|x\rangle$ . The red bars indicate the experimental or HHL simulated results for the state amplitudes. The states haven't been normalized so that deviation from the solution of the original linear equation system can be prominently noticed.

MHRD for their support. B.K.B. acknowledges the financial support of IISER Kolkata. The authors acknowledge the support of the Qiskit SDK in enabling us to simulate the quantum circuits. They appreciate the assistance received from Charles Moussa (Oak Ridge National Lab,

Tennessee) in comprehending the intricacies of the Group Leaders Optimization algorithm. They are also grateful for all the help received from the members of the Stack Exchange and Qiskit communities, in various stages of the project.

## References

- [1] M. A. Nielsen and I. L. Chuang, *Quantum Computation and Quantum Information: 10th Anniversary Edition*, 10th ed. (Cambridge University Press, NY, USA, 2011).
- [2] S. Lloyd, *Science* **273**, 1073 (1996).
- [3] D. Aharonov and A. Ta-Shma, in *Proceedings of the Thirty-fifth Annual ACM Symposium on Theory of Computing, STOC'03* (ACM, NY, USA, 2003) pp.20–29.
- [4] A. W. Harrow, A. Hassidim, and S. Lloyd, *Phys. Rev. Lett.* **103**, 150502 (2009).
- [5] L. Hales and S. Hallgren, in *Foundations of Computer Science, 2000. Proceedings. 41st Annual Symposium on* (IEEE, 2000) pp. 515-525.
- [6] E. Farhi, J. Goldstone, and S. Gutmann, arXiv preprint arXiv:1411.4028 (2014).
- [7] A. Peruzzo, J. McClean, P. Shadbolt, M.-H. Yung, X.-Q. Zhou, P. J. Love, A. Aspuru-Guzik, and J. L. O'Brien, *Nature commun.* **5**, 4213 (2014).
- [8] A. Kandala, A. Mezzacapo, K. Temme, M. Takita, M. Brink, J. M. Chow, and J. M. Gambetta, *Nature* **549**, 242 (2017).
- [9] K. Srinivasan, S. Satyajit, B. K. Behera, and P. K. Panigrahi, arXiv e-prints (2018), arXiv:1805.10928 [quant-ph].

- [10] A. Dash, D. Sarmah, B. K. Behera, and P. K. Panigrahi, arXiv e-prints (2018), arXiv:1805.10478 [quant-ph].
- [11] K. Srinivasan, B. K. Behera, and P. K. Panigrahi, arXiv e-prints (2018), arXiv:1801.00778 [quant-ph].
- [12] J. Friedman, T. Hastie, and R. Tibshirani, *The elements of statistical learning*, Vol. 1 (Springer series in statistics New York, NY, USA:, 2001).
- [13] J. Biamonte, P. Wittek, N. Pancotti, P. Rebentrost, N. Wiebe, and S. Lloyd, *Nature* **549**, 195 (2017).
- [14] A. M. Childs, R. Kothari, and R. D. Somma, *SIAM J. Comput.* **46**, 1920 (2017).
- [15] D. Dervovic, M. Herbster, P. Mountney, S. Severini, N. Usher, and L. Wossnig, arXiv e-prints (2018), arXiv:1802.08227 [quant-ph].
- [16] Adrien Suau. (2018, November 8). nelimee/quantum-hhl-4x4: Working 4x4 HHL implementation (Version v1.0.0). Zenodo. <http://doi.org/10.5281/zenodo.1480661>
- [17] J. Pan, Y. Cao, X. Yao, Z. Li, C. Ju, H. Cheng, X. Peng, S. Kais, J. Du, "Experimental realization of quantum algorithm for solving linear systems of equations" *Phys. Rev. A* **89**, 022313 (2014)
- [18] Y. Cao, A. Daskin, S. Frankel, and S. Kais, *Mol. Phys.* **110**, 1675 (2012), arXiv:1110.2232v2 [quant-ph].
- [19] M. R. Hestenes and E. Stiefel, *Methods of conjugate gradients for solving linear systems*, Vol. 49 (NBS Washington, DC, 1952).
- [20] A. Ambainis, arXiv e-prints (2010), arXiv:1010.4458 [quant-ph].
- [21] L. Wossnig, Z. Zhao, and A. Prakash, *Phys. Rev. Lett.* **120**, 050502 (2018).
- [22] P. B. Buhlmann and S. Van De Geer, *Statistics for high-dimensional data: methods, theory and applications* (Springer Science & Business Media, 2011).
- [23] A. Daskin and S. Kais, *Mol. Phys.* **109**, 761 (2011), arXiv:1004.2242.
- [24] E. Jones *et al.*, "Scipy: Open source scientific tools for Python," (2001).
- [25] J. Nocedal and S. J. Wright, *Numerical Optimization*, 2nd ed. (Springer, 2006).
- [26] A. Daskin and S. Kais, *J. Chem. Phys.* **134**, (2011).
- [27] A. Al-Mohy and N. Higham, *SIAM Journal on Matrix Analysis and Applications*, **31**, 970, (2010).
- [28] N. Higham, *SIAM Journal on Matrix Analysis and Applications* **26**, 1179 (2005)
- [29] Matlab Mathematics R2018b, The MathWorks, Inc., Natick, Massachusetts, United States.
- [30] C. Moler and C. Van Loan, *SIAM Review* **45**, 3 (2003).
- [31] J. Niesen and W. M. Wright, *ACM Trans. Math. Softw.* **38**, 221 (2012).
- [32] A. Al-Mohy and N. Higham, *SIAM Journal on Scientific Computing* **33**, 488 (2011).
- [33] M. A. Nielsen, "Cluster-state quantum computation." *Reports on Mathematical Physics* **57**, 147 (2006).
- [34] G. Marsaglia, "Xorshift RNGs" *Journal of Statistical Software*, **8** 1 (2003)
- [35] S. Marsland, "Machine Learning" CRC Press, §4.1.1. (2011)



## Supplementary Material

### I. Group Leaders Optimization Algorithm

The Group Leaders Optimization Algorithm (GLOA) is a genetic algorithm which was developed by Anmer Daskin and Sabre Kais in 2010 [1]. One of the primary applications of the algorithm is to find low cost quantum gate sequences to closely approximate any unitary operator [2]. Generally speaking, the advantage of genetic algorithms compared to other optimization techniques is that they don't get stuck in local extremas. We will briefly discuss the algorithm here, in the context of quantum gate decomposition.

**Step I:** For any arbitrary unitary operator  $\mathbf{U}_t$ , consider a set (of considerable size) of gates out of the basic  $R_x, R_y, R_z, R_{zz}$ , Pauli- $X$ , Pauli- $Y$ , Pauli- $Z$ ,  $V$  (square root of Pauli- $X$ ),  $V^\dagger$ ,  $S$  ( $\frac{\pi}{8}$  gate),  $T$  ( $\frac{\pi}{4}$  gate) and  $H$  gates along with their controlled counterparts (refer to the Appendix of [1] for matrix representations of these gates). Which gate set is to be chosen depends on the context and the choice might directly affect the efficiency, precision and convergence time of the algorithm. One usually tries to choose a universal set of quantum gates. Each gate in the chosen gate set is assigned an index from 1 onwards. For example, if our gate set were  $\{V, Z, S, V^\dagger\}$  we could have numbered them as  $V = 1, Z = 2, S = 3$  and  $V^\dagger = 4$ . For this algorithm, any single qubit gate can be represented as a four-parameter string in the form  $\langle \text{index number of gate} \rangle \langle \text{index of target qubit} \rangle \langle \text{index of control qubit} \rangle \langle \text{angle of rotation} \rangle$ . The index number of the control and target qubits can vary from 1 to total number of qubits (on which  $\mathbf{U}$  acts) and the angle of rotation can vary from 0 to  $2\pi$ . The angle of rotation is represented by positive floating point numbers whereas the indices are represented by natural numbers. The total number of gates in the decomposition is termed as  $\max_{\text{gates}}$ , which is restricted to a maximum of 20 in the GLOA. Say the total number of gates in the decomposition is considered to be say  $m$ , then the corresponding  $4m$ -parameter string representing the circuit would be of the form  $\langle \text{gate}_1 \rangle \langle \text{t.q}_1 \rangle \langle \text{c.q}_1 \rangle \langle \text{angle}_1 \rangle \langle \text{gate}_2 \rangle \langle \text{t.q}_2 \rangle \langle \text{c.q}_2 \rangle \langle \text{angle}_2 \rangle \dots \langle \text{gate}_m \rangle \langle \text{t.q}_m \rangle \langle \text{c.q}_m \rangle \langle \text{angle}_m \rangle$ , where t.q and c.q are abbreviations for 'target qubit' and 'control qubit' respectively.

**Step II:**  $n$  groups of  $p$  such randomly generated  $4 \times \max_{\text{gates}}$ - parameter strings are created. The groups now look as in figure 1. It is important to emphasize that the entire  $n \times p$  population of strings is randomly generated, following the constraints on the index numbers (as described in Step I) and angles (the decimal representing an angle can range from 0 to  $2\pi$  only).

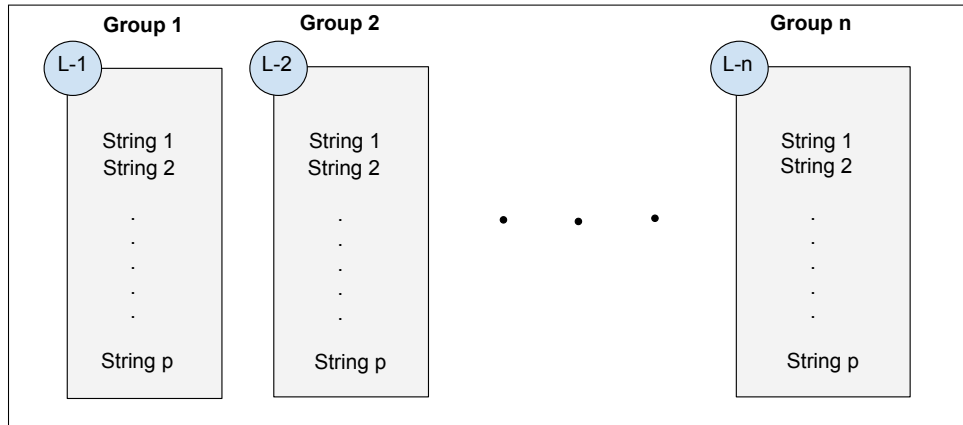


FIG. 1. In Step II of the algorithm  $n$  groups of  $p$  randomly generated member strings are created. In step III the leader strings L-1, L-2,..., L-n are chosen for each group on basis of their trace fidelities.

**Step III:** For the matrix operator equivalent of any such member string i.e.,  $\mathbf{U}_a$ , we can calculate the value of trace fidelity  $\mathcal{F}$ , which is defined as

$$\frac{1}{N} |\text{Tr}(\mathbf{U}_t \mathbf{U}_a^\dagger)|$$

where  $\mathbf{U}_t$  is the operator corresponding to the unitary circuit which we are trying to approximate. It is a measure of the *closeness* of the two operators  $\mathbf{U}_a$  and  $\mathbf{U}_t$ . The values of  $\mathcal{F}$  can only lie in  $[0, 1]$ . This is because the product of two unitary matrices is always unitary and furthermore all eigenvalues of unitary matrices have a magnitude of 1

and that the trace of a square matrix is the sum of its eigenvalues. We can clearly see that higher the value of  $\mathcal{F}$ , the greater is the closeness of  $\mathbf{U}_a$  and  $\mathbf{U}_t$ . And when  $\mathbf{U}_a = \mathbf{U}_t$ , the trace fidelity is unity. Using this definition, we calculate the trace fidelities of all the  $n \times p$  number of member strings. In each of the  $n$  groups, the string having the highest value of trace fidelity is considered to be the leader of that group. So we get  $n$  leader strings in each run.

**Step IV:** In this step we mutate every parameter (element) of all the member strings using a weighted sum involving the original string, the leader string and a randomly generated string. Each parameter  $pr$  ( $1 \leq pr \leq 4 \times \max_{\text{gate}}$ ) of a member string in any group is modified following the rule:

$$\text{new string}_{ij}[pr] = r_1 \times \text{member string}_{ij}[pr] + r_2 \times \text{leader string}_i[pr] + r_3 \times \text{random string}_{ij}[pr].$$

The subscript  $i, j$  indicates the  $i$ -th member of the  $j$ -th group ( $1 \leq i \leq n$  and  $1 \leq j \leq p$ ). Since the leader string is shared by all members of a particular group, we use only the single index subscript  $i$  for it.  $\text{random string}_{ij}$  represents a randomly generated string corresponding to the  $i$ -th member string of the  $j$ -th group. Here  $r_1 + r_2 + r_3 = 1$  and in general the best results are obtained when  $r_1 = 0.8$  and  $r_2, r_3$  are considered to be 0.1 each. We summarize this step with the following pseudo-code:

```

for  $i = 1$  to  $n$  do
  for  $j = 1$  to  $p$  do
    for  $pr = 1$  to  $4 \times \max_{\text{gate}}$  do
       $\text{new string}_{ij}[pr] = r_1 \times \text{member string}_{ij}[pr] + r_2 \times \text{leader string}_i[pr] + r_3 \times \text{random string}_{ij}[pr]$ 
    end for
    if  $\text{fidelity}(\text{new string}_{ij})$  is greater than  $\text{fidelity}(\text{member string}_{ij})$  then
       $\text{member string}_{ij} = \text{new string}_{ij}$ 
    end if
  end for
end for

```

**Step V:** In this step we perform one-way crossovers, also known as parameter transfer. The (randomly chosen)  $pr$ -th parameter of any random member string  $k$  belonging to a group  $i$  is replaced with the  $pr$ -th parameter of  $k$  member of a randomly chosen group  $x$ . It is necessary to keep in mind that only if the trace fidelity of this new string generated after crossover is greater than the original fidelity, the original member string is replaced. This is repeated  $t$  times for each group (not for each member).  $t$  is a random positive integer bounded above by  $\frac{4 \times \max_{\text{gate}}}{2} - 1$ . The pseudo-code is as follows:

```

for  $i = 1$  to  $n$  do
   $t = \text{random}(\frac{4 \times \max_{\text{gate}}}{2} - 1)$ 
  for  $j = 1$  to  $t$  do
     $x = \text{random}(n)$ 
     $k = \text{random}(p)$ 
     $pr = \text{random}(4 \times \max_{\text{gate}})$ 
     $\text{new string}_{ik}[pr] = \text{member string}_{xk}[pr]$ 
    if  $\text{fidelity}(\text{new string}_{ik})$  is greater than  $\text{fidelity}(\text{member string}_{ik})$  then
       $\text{member string}_{ik} = \text{new string}_{ik}$ 
    end if
  end for
end for

```

In the pseudo-code, the **random(x)** function is basically a function which randomly generates a positive integer bounded by  $x$ . Fast pseudo-random generators such as Xorshift [3] or Mersenne twisters [4] may be utilized for this purpose.

**Step VI:** The fidelities are re-calculated for all the strings in all the groups. In case the fidelity of any of the leader strings surpasses the desired fidelity threshold, the algorithm is terminated and that string with the highest fidelity

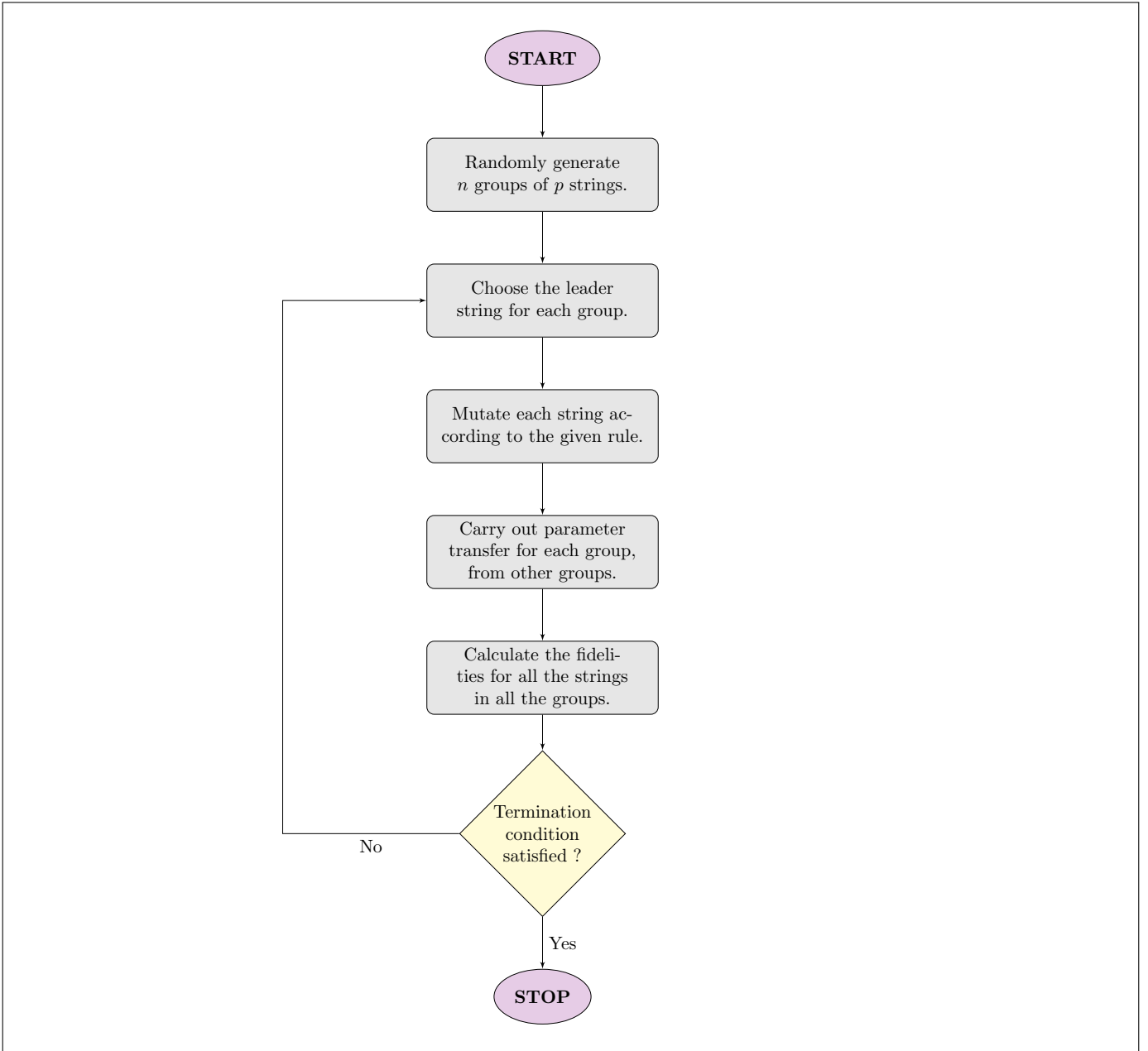


FIG. 2. A flowchart representing the steps of the Group Leaders Optimization algorithm

(in the whole population) is returned. We might also terminate the algorithm once a desired number of iterations are completed - say 10,000.

## II. Exact Gate Decomposition of the Hamiltonian Simulation Step

Any  $4 \times 4$  two-qubit Hamiltonian, which may be represented as a  $4 \times 4$  matrix, can be easily decomposed into the four basic Pauli matrices  $\sigma_1 = \mathbb{I}, \sigma_x = X, \sigma_y = Y, \sigma_z = Z$ . Say we want to express our two-qubit Hamiltonian  $\mathbf{H}$  in the form

$$\mathbf{H} = \sum_{i,j=1,x,y,z} a_{i,j}(\sigma_i \otimes \sigma_j).$$

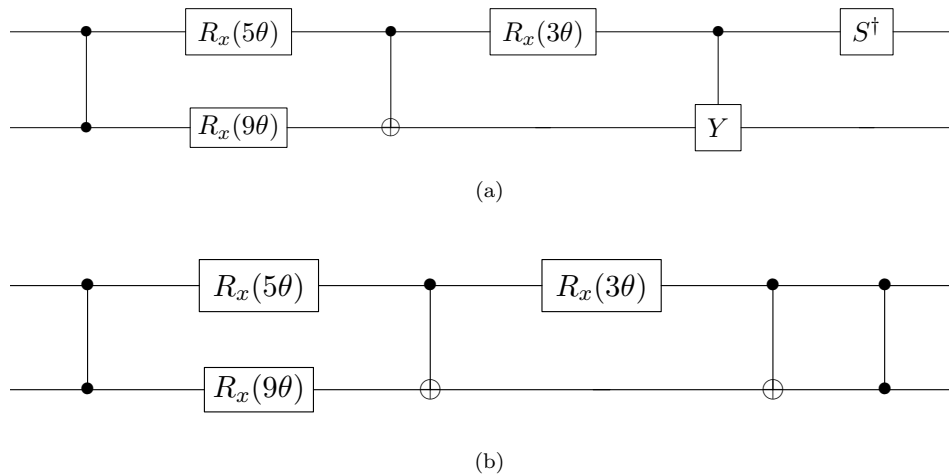


FIG. 3. (a) shows the exact gate decomposition for  $e^{i\mathbf{A}t}$ . (b) is a simplified version of (a) obtained by combining the two controlled gates at the end.

Then the coefficients  $a_{i,j}$  turn out to be

$$a_{i,j} = \frac{1}{4} \text{Tr}[(\sigma_i \otimes \sigma_j) \mathbf{H}].$$

The factor of  $\frac{1}{4}$  is meant to normalize the Pauli matrices, since  $\|\sigma_i\| = \sqrt{\text{Tr}[\sigma_i^\dagger \sigma_i]} = \sqrt{2}$ . Using this technique, the Pauli decomposition of the  $4 \times 4$  matrix  $\mathbf{A}$  i.e.

$$\mathbf{A} = \frac{1}{4} \begin{bmatrix} 15 & 9 & 5 & -3 \\ 9 & 15 & 3 & -5 \\ 5 & 3 & 15 & -9 \\ -3 & -5 & -9 & 15 \end{bmatrix} \quad (1)$$

turns out to be<sup>1</sup>

$$\mathbf{A} = \frac{1}{4} (15\mathbb{I} \otimes \mathbb{I} + 9Z \otimes X + 5X \otimes Z + 3Y \otimes Y).$$

Neglecting the scaling factor of  $\frac{1}{4}$ , we note that each one of the terms commute, which implies

$$e^{i\mathbf{A}\theta} = e^{15i\theta} e^{9i\theta Z \otimes X} e^{5i\theta X \otimes Z} e^{3i\theta Y \otimes Y}.$$

Another observation is that the commuting terms are the stabilizers of the 2-qubit cluster state [5]. So we attempt to use controlled phase gates to get the correct terms. We can rotate the first qubit about the  $x$ -axis by an angle  $5\theta$  and the second qubit about the  $x$ -axis by angle  $9\theta$ . The structure of  $e^{3i\theta X \otimes X}$  is a  $x$ -rotation on the computational basis states  $\{|00\rangle, |11\rangle\}$  and another on  $\{|01\rangle, |10\rangle\}$ . A CNOT gate converts these bases into single qubit bases, controlled off the target qubit. Since both implement the same rotation but controlled off opposite values, we can remove the control. The overall circuit is shown in figure 3a, which can be further simplified by combining the two controlled gates at the end as in figure 3b.

[1] A. Daskin and S. Kais, Mol. Phys. **109**, 761 (2011), arXiv:1004.2242.

[2] A. Daskin and S. Kais, J. Chem. Phys. **134**, (2011).

[3] G. Marsaglia, "Xorshift RNGs" Journal of Statistical Software, **8** 1 (2003)

[4] S. Marsland, "Machine Learning" CRC Press, §4.1.1. (2011)

[5] M. A. Nielsen, "Cluster-state quantum computation." Reports on Mathematical Physics **57**, 147 (2006).

<sup>1</sup> Courtesy of Dr. Alastair Kay (Royal Holloway, University of London), who also designed the quantum circuits in figures 3a and 3b.